24th COBEM - 2017

24th ABCM International Congress of Mechanical Engineering
December 3-8, 2017, Curitiba, PR, Brazil

COBEM-2017-1770
PERTURBATION OF A TURBULENT CHANNEL FLOW BY A TWO-DIMENSIONAL TRIANGULAR RIPPLE

Fernando David Cúñez Benalcázar
Erick de Moraes Franklin
University of Campinas, School of Mechanical Engineering, Rua Mendeleyev, 200, Campinas, 13083-970, Brazil
fernandodcb@fem.unicamp.br, franklin@fem.unicamp.br

Abstract. *Turbulent flows perturbed by low hills are commonly found in industrial and environmental applications. The perturbation introduces new scales in the problem changing the main flow properties along the hills. This study presents an experimental study on a perturbation of fully-developed turbulent channel flow by a triangular ripple. Two water flows that correspond to Reynolds numbers of 27,500 and 35,000 were imposed over an asymmetric triangular hill fixed on the bottom wall of a rectangular closed conduit, and the flow fields were measured by PIV (Particle Image Velocimetry). From the instantaneous flow fields, the mean velocities and fluctuations were computed, and the shear stress over the ripple and the field of turbulent production were determined. The general behaviors of obtained velocities and stresses are compared to published asymptotic analyses and the shear stress is discussed in terms of bed stability.*

Keywords: *Turbulent Flows, Turbulent Boundary Layer, Perturbation, PIV.*

1. INTRODUCTION

Turbulent boundary layers perturbed by hills are frequently found in nature and industry. Some examples are the airflows over hills, ocean waves and desert dunes, and also water flows over aquatic dunes (which have a triangular profile) inside closed conduits. The latter is commonly encountered in industrial applications, such as petroleum pipelines, dredging lines and sewer systems. The perturbation of the turbulent boundary layer introduces new scales in the problem, changing the velocity and the stress distributions along the hill. These changes are of importance for many environmental and industrial applications. For example, to understand the bed instabilities associated with sediment transport. Over the last years, many studies have been devoted to the perturbation of a two-dimensional turbulent boundary layer by a low hill (Jackson and Hunt, 1975; Hunt *et al.*, 1988; Belcher and Hunt, 1998; Franklin and Ayek, 2013), some of them, based on asymptotic methods, have improved our knowledge on the subject. The majority of these studies have investigated flows with high Reynolds numbers. In the case of moderate Reynolds numbers (approximately 10^4), there is a lack of experimental results for the perturbation of turbulent channel flows by triangular ripples. For example, Franklin and Ayek (2013) studied the evolution of the shear stress along a triangular profile. Their experimental results showed that the flow is not in local-equilibrium conditions along the upstream face of the ripple.

This paper presents an investigation on the perturbation of a two-dimensional fully-developed turbulent flow by a triangular ripple. Two water flows were imposed over an asymmetric triangular hill fixed on the bottom wall of a closed conduit and the flow field was measured by PIV (Particle Image Velocimetry). From the instantaneous flow fields, the mean velocities and fluctuations were computed. The obtained velocities and stresses are compared to published asymptotic analyses and the surface shear stress is discussed in terms of instabilities of a granular bed.

2. EXPERIMENTAL PROCEDURE

The experimental device consisted basically of a water reservoir, two centrifugal pumps, a flow meter, a flow straightener, 5m long rectangular transparent channel (160mm wide by 50mm high), a settling tank, and a return line, so that the water flowed in a closed loop following the above order of description. Figure 1 presents a layout of the experimental device.

Two flow rates were employed, 8 and 10 m^3/h, corresponding to cross-section mean velocities $\overline{U}$ = 0.32 and 0.40m/s and to Reynolds numbers $Re = (2\overline{U}H_{eff}/\nu)$ of 27,500 and 35,000, where H_{eff} is the distance from the surface of the PVC plates to the top wall of the channel. The regime was hydraulically smooth in all the cases. PVC plates of $7mm$ thickness were inserted in the channel, covering its entire bottom and reducing its height to $43mm$. To model the triangular ripple, a small bed-form of triangular shape was fixed on a PVC plate in the test section. This triangular bed-form had the same scales as the aquatic ripples usually found in environmental and industrial applications. Measurements

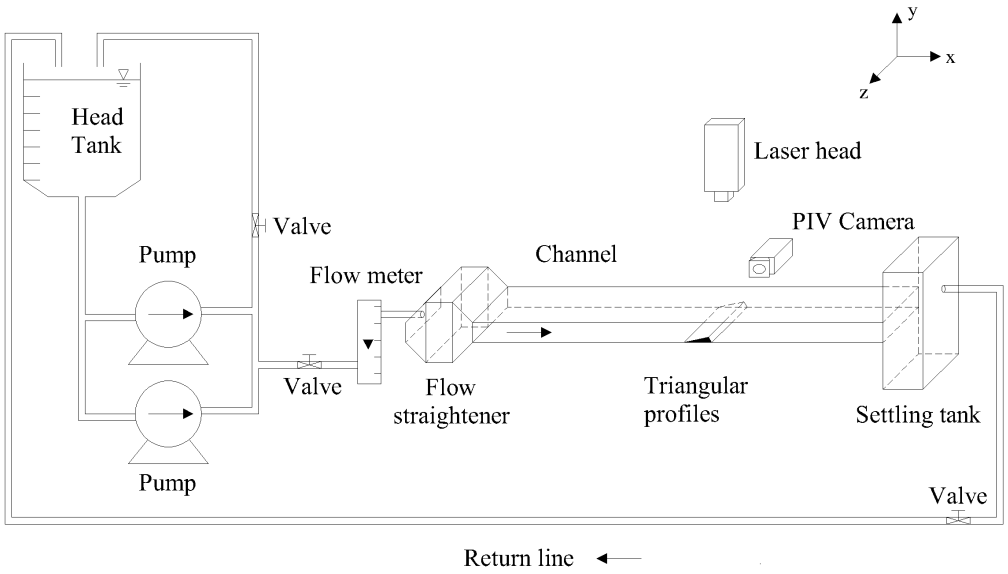

Figure 1. Layout of the experimental device

were performed without and with the ripple in the closed conduit and were taken at the vertical symmetry plane of the channel. To obtain the instantaneous velocity fields of the flow, we used PIV (Particle Image Velocimetry). The employed light source was a dual cavity Nd:YAG Q-Switched laser, capable to emit $2\times130mJ$ at $15Hz$ pulse rate. The power of the laser was fixed at 66% of the maximum power to assure a good balance between the image contrasts and undesirable reflection from the channel walls. $10\mu m$ hollow glass beads (S.G. = 1.05) were employed as seeding particles. To capture the images, we used a $7.4\mu m \times 7.4\mu m$ (px^2) CCD (charge coupled device) camera with a spatial resolution of 2,048px $\times$ 2,048px and acquiring pairs of images at $4Hz$. The test section was divided in four parts, for each part were acquired 2,000 pairs of images for both flow rates. Fields of instantaneous velocity were computed in fixed Cartesian grids by the PIV controller software (DaVis). MatLab scripts were written to post-process these fields.

3. RESULTS AND DISCUSSION

The first tests were made upstream of the bed form. In this part, the flow corresponded to a fully-developed turbulent channel flow. We encountered the typical characteristics of a fully-developed turbulent channel flow, such as the logarithmic region for the bottom and top walls ($70 < y^+ < 200$, where y^+ is the dimensionless vertical coordinate, $y^+ = yu_*/\nu$, with u_* being the shear velocity, and ν the kinematic viscosity) by considering a hydraulic smooth regime, and the typical profiles of the xy component of the Reynolds stress.

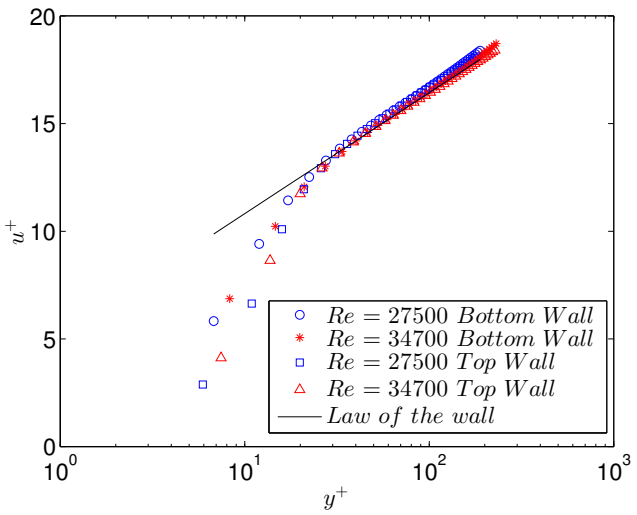

Figure 2. Mean velocity profiles.

Figure 2 presents the log-normal profiles of the mean velocities for the two flow rates. The abscissa is in logarithmic scale and represents the vertical distance from the channel walls walls (bottom or top) normalized by the viscous length, y^+ . The ordinate is in linear scale and corresponds to the mean velocities normalized by the shear velocity, $u^+ = u/u_*$.

The same flow rates were used for the flow over the triangular ripple. Figure 3 allows us to distinguish the different regions of the flow field. From this figure, we see that the perturbed flow has at least three distinct regions: (i) one far from the ripple surface where the $v \approx 0$ and the perturbation in u is small (given mainly by confinement effects); (ii) other close to the ripple surface and downstream of the crest, where a recirculation bubble exists; (iii) and a third one close to the ripple surface and upstream of the crest, where v is directed upwards and the perturbation of u is stronger than far from the bed.

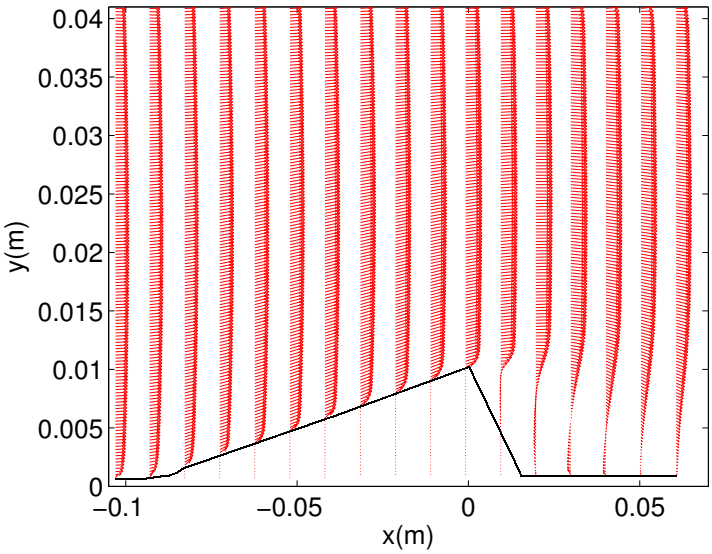

Figure 3. Some profiles of the perturbed mean velocities over the triangular ripple. The flow is from left to right and $Re = 27,500$.

Figure 4 presents some profiles of the xy aligned component of the Reynolds stresses with respect to the triangular ripple surface in dimensionless form, usptream of the ripple crest. This figure shows that the xy component of the Reynolds stresses -$\overline{u'_\theta v'_\theta}$ is perturbed in the $50 < y_d^+ < 250$ region (where y_d^+ is the dimensionless vertical displaced coordinate, $y_d^+ = y_d u_*/\nu$, with y_d being the vertical displaced coordinate defined as $y_d = y - h$, where h is the local height of the ripple) that corresponds to the overlap layer of the unperturbed boundary layer, If the flow is in local equilibrium in the $y_d^+ < 250$ region, the shear stress on the surface $\rho u_{*,0}^2$ shall scale with -$\overline{u'_\theta v'_\theta}$.

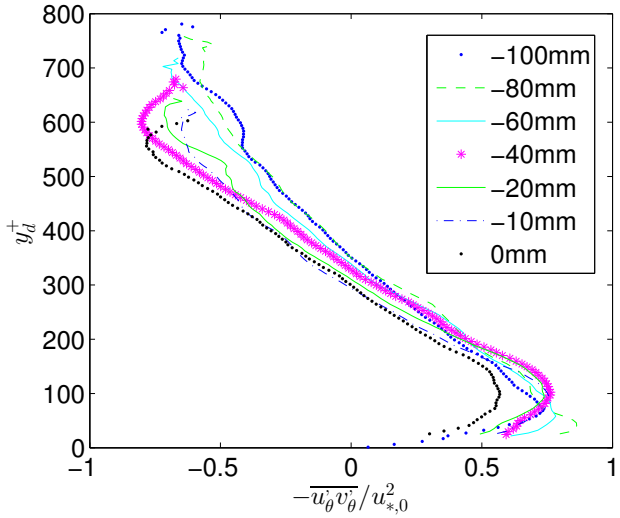

Figure 4. Some profiles of the xy component of the Reynolds stress in dimensionless form: y_d^+ versus -$\rho\overline{u'_\theta v'_\theta}/(\rho u_{*,0}^2)$ upstream of the ripple crest. $Re = 27,500$.

The experimental data for -$\overline{u'_\theta v'_\theta}$ had considerable noise. To decrease the noise, the obtained -$\overline{u'_\theta v'_\theta}$ profiles were averaged by a sliding window process over the closest nine points.

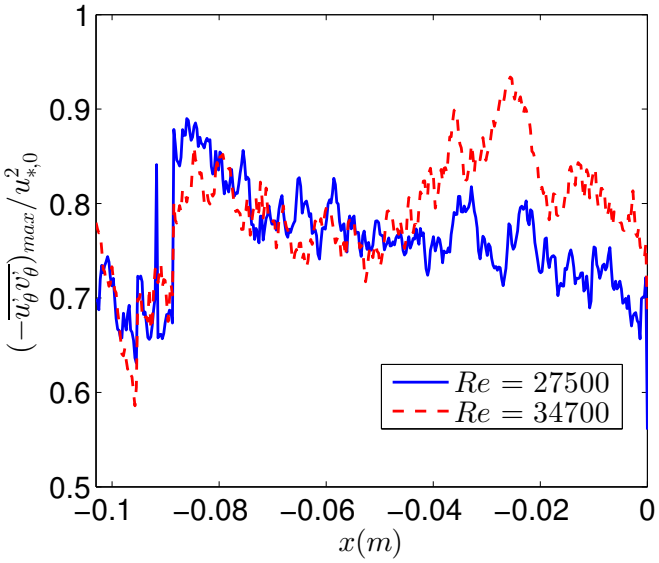

Figure 5. Maximum normalized Reynolds stress $(-\overline{u'_\theta v'_\theta})_{max}/(u^2_{*,0})$ as a function of the longitudinal position x. The *continuous* and *dashed lines* correspond to Re = 2.75×10^4 and Re = 3.5×10^4, respectively.

Figure 5 presents the longitudinal evolution of the maximum of the *xy* aligned component of the Reynolds stress $(-\overline{u'_\theta v'_\theta})_{max}$ (for each vertical profile) normalized by $u^2_{*,0}$, for the bottom wall region. Figure 5 shows (for each case) that $(-\overline{u'_\theta v'_\theta})_{max}$ increases approximately *30%* where the triangular ripple starts at x ≈-0.09m. For Re = 2.75×10^4, $(-\overline{u'_\theta v'_\theta})_{max}$ decreases in the 0.09$m \leq x \leq$ 0m region until $(-\overline{u'_\theta v'_\theta})_{max} \approx 0.65 u^2_{*,0}$. For Re = 3.5×10^4, $(-\overline{u'_\theta v'_\theta})_{max}$ has a different behavior in the 0.09$m \leq x \leq$ 0m region. This cannot be asserted because of the relatively high noise in the data. However we obtain that $(-\overline{u'_\theta v'_\theta})_{max} \sim O(u_{*,0}{}^2)$ in the region analyzed. This indicates that, for the water flow over a triangular ripple (for each case), the region corresponding to the overlap sublayer of the unperturbed flow is in local equilibrium with the lower sublayers.

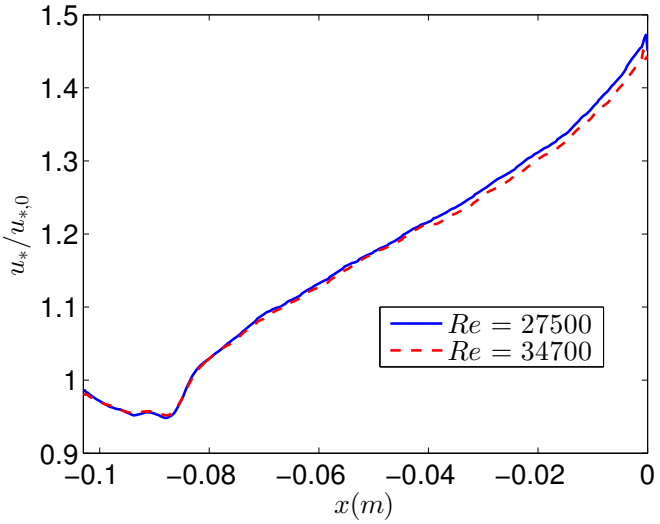

Figure 6. Normalized local shear velocity $u_*/u_{*,0}$ as a function of longitudinal position x, upstream of the ripple crest. The *continuous* and *dashed lines* correspond to Re = 2.75×10^4 and Re = 3.5×10^4, respectively.

Based on the local-equilibrium assumptions, we computed the local shear velocity for the perturbed flow u_*, by fitting each mean velocity profile along the ripple, with a logarithmic curve. Figure 6 presents the local shear velocity normalized by the shear velocity of the unperturbed flow, $u_*/u_{*,0}$ as a function of longitudinal position x, for both flow rates. We used a smooth spline interpolation to decrease the noise in the results. From this figure, we observe that the shear velocity decreases at the beginning of the ripple and then increases to a value approximately 1.4 times $u_{*,0}$ for both cases. The

general behavior of the longitudinal evolution of normalized shear velocity is consistent with measurements of turbulent boundary layers over dunes in a desert, where local-equilibrium conditions in inner regions are evident (Andreotti *et al.*, 2002; Sauermann *et al.*, 2003).

4. CONCLUSIONS

This paper experimentally studied the perturbation of a turbulent boundary layer by a two-dimensional triangular ripple, in the hydraulic smooth regime. The experiments were performed with water flows in moderate Reynolds numbers (10,000 < Re < 50,000). The flow was measured by PIV, from which the instantaneous and mean velocity fields could be obtained. These velocity fields were post-processed, allowing us to determinate the general behaviors of the perturbed and unperturbed turbulent flow.

Some of the main aspects of the turbulent flow over a low ripple were confirmed by the experimental results: a recirculation bubble is formed downstream of the ripple crest, and the aspect ratio of recirculation bubble for each flow rate is coherent with the literature. Along the upstream face of the ripple, the maxima of the xy component of the Reynolds stresses is of the same order of magnitude of the square of the unperturbed shear velocity. In addition, the maxima of the $-\overline{u'v'}$ profiles decrease slightly in the longitudinal direction towards the crest of the ripple in the layer corresponding to the overlap layer. Based on these characteristics, it seems that the flow is in local equilibrium in this region.

In this work, we also computed the local shear velocity for the perturbed flow u_* along the ripple by assuming local-equilibrium conditions from the upstream leading edge until the ripple crest. The values of u_* decrease slightly at the leading edge of the ripple and increase significantly towards the ripple crest, reaching a value 40% higher at the crest than the unperturbed value.

5. ACKNOWLEDGEMENTS

Fernando David Cúñez Benalcázar is grateful to SENESCYT (Programa de Becas Convocatoria Abierta 2014 Segunda Fase) and to FAPESP (grant no. 2016/18189-0), Erick de Moraes Franklin is grateful to FAPESP (grant no. 2012/19562-6 and 2016/13474-9) and to CNPq (grant no. 400284/2016-2) for the financial support they provided.

6. REFERENCES

Andreotti, B., Claudin, P. and Douady, S., 2002. "Selection of dune shapes and velocities. part 1: Dynamics of sand, wind and barchans". *The European Physical Journal B-Condensed Matter and Complex Systems*, Vol. 28, pp. 321–329.

Belcher, S.E. and Hunt, J.C.R., 1998. "Turbulent flow over hills and waves". Vol. 30, pp. 507–538.

Franklin, E.M. and Ayek, G.A., 2013. "The perturbation of a turbulent boundary layer by a two-dimensional hill". *Journal of the Brazilian Soc. Mechanical Sciences*, Vol. 35, pp. 337–346.

Hunt, J.C.R., Leibovich, S. and Richards, K., 1988. "Turbulent shear flows over low hills". *Quart. J. R. Met. Soc.*, Vol. 114, pp. 929–955.

Jackson, P.S. and Hunt, J.C.R., 1975. "Turbulent wind flow over a low hill". *Quart. J. R. Met. Soc.*, Vol. 101, pp. 1435–1470.

Sauermann, G., Andrade, J.S., Maia, L.P., Costa, U.M.S., Araújo, A.D. and Herrmann, H.J., 2003. "Wind velocity and sand transport on a barchan dune". *Geomorphology*, Vol. 54, pp. 245–255.

7. RESPONSIBILITY NOTICE

The following text, properly adapted to the number of authors, must be included in the last section of the paper:
The author(s) is (are) the only responsible for the printed material included in this paper.